Perfect-Reconstruction Cosine-Modulated Filter Banks via Improved Constraint Linearization

Wu-Sheng Lu
Dept. of Electrical and Computer Engineering
University of Victoria, Victoria, BC, Canada
Email: wslu@ece.uvic.ca

Takao Hinamoto
Hiroshima University
Higashi-Hiroshima, 739-8527, Japan
Email: hinamoto@ieee.org

Tapio Saramäki
Dept. of Signal Processing
Tampere University of Technology
Tampere, Finland
tapio.saramaki@tut.fi

***Abstract*—The design of perfect-reconstruction cosine-modulated filter banks is revisited by applying new linearization techniques for the time-domain quadratic perfect reconstruction constraints. The new techniques are analyzed to explain why they can provide improved approximation accuracy hence improved performance with insignificant increase in complexity. A design example is presented for performance demonstration and comparison.**

I. Introduction

M-channel cosine-modulated filter banks (CMFBs) find many applications ranging from audio signal processing to subband coding of images. From an implementation perspective, CMFBs are preferred to quadrature mirror filtering techniques as the former can be implemented using fast discrete cosine transforms and the number of parameters involved is considerably smaller.

The theory of M-channel CMFBs has been well understood and methods for the design of CMFBs are abundant, see for example [1]–[18] and the references therein. CMFBs are usually classified as biorthogonal and orthogonal cosine-modulated filter banks that maintain perfect reconstruction (PR) or near perfect reconstruction property. For the sake of detailed exposition of the design technique in limited space, this paper focuses on the design of PR uniform orthogonal CMFBs. Nevertheless, the proposed design technique is directly applicable to other classes of CMFBs mentioned above with straightforward modifications. We also remark that the proposed design technique shall enable improved design of nonuniform CMFBs that are derived by merging adjacent filters from a uniform CMFB [19].

The design technique presented in this paper is closely related to those developed in [14] and [18] which have proven effective for large-scale (in number of channels and length of individual filters) PR CMFBs in terms of approximation accuracy and computational complexity. In essence, references [14] and [18] take an approach where the stopband energy of the prototype filter is minimized subject to a set of time-domain quadratic algebraic equations. These equations are imposed in order for the CMFB to hold PR property. On the other hand, the presence of these equality constraints leads to a *nonconvex* quadratic programming (QP) problem which admits multiple suboptimal solutions and, therefore, presents significant technical challenges when seeking satisfactory designs. A key step taken in both [14] and [18] is to linearize the quadratic constraints so that in each iteration of the design one deals with a standard *convex* QP problem and, when the iterates converge, asymptotically the linearized constraints become equivalent to the original set of quadratic equations and hence the converging solution is expected to hold the PR property with high accuracy. In this paper the aforementioned step is enhanced by using a more accurate linear approximation. This results in an improved design algorithm with practically the same computational complexity as that of [18].

The paper is organized as follows. Sec. II provides necessary background of CMFBs, especially the class of PR orthogonal CMFBs. This is followed by a QP formulation of the design problem at hand. Sec. III presents an analysis of convexifying the QP problem and proposes new linearization schemes for the quadratic time-domain constraints. The design algorithm based on the new linearization technique is then summerized. A design example is presented in Sec. IV for performance evaluation and comparison, and concluding remarks are made in Sec. V.

II. Perfect-Reconstruction Cosine-Modulated Filter Banks

An M-channel, maximally decimated biorthogonal cosine-modulated filter bank is characterized by the impulse responses of its analysis and synthesis filters as

$$h_k(n) = 2p(n)\cos\left[\frac{\pi}{M}(k+\frac{1}{2})(n-\frac{D}{2})+(-1)^k\frac{\pi}{4}\right]$$

and

$$g_k(n) = 2p(n)\cos\left[\frac{\pi}{M}(k+\frac{1}{2})(n-\frac{D}{2})-(-1)^k\frac{\pi}{4}\right]$$

where $k = 0,\ 1,\ \ldots,\ M-1$ and $n = 0,\ 1,\ \ldots,\ N-1$; $\{p(n)$ for $n = 0,\ 1,\ \ldots,\ N-1\}$ is the impulse response of the FIR *prototype filter* (PF); and D is the system delay. The input-output relation of the CMFB in the z domain is given by

$$Y(z) = T_0(z)X(z) + \sum_{l=1}^{M-1} T_l(z)X(ze^{-j2\pi l/M})$$

where

$$T_0(z) = \frac{1}{M}\sum_{k=0}^{M-1} G_k(z)H_k(z)$$

and

$$T_l(z) = \frac{1}{M}\sum_{k=0}^{M-1} G_k(z)H_k(ze^{-j2\pi l/M})$$

are the distortion and alias transfer functions which respectively determine the distortion caused by the system for unaliased component $X(z)$ and how the aliased components $X(ze^{-j2\pi l/M})$ are attenuated. Consequently, the CMFB holds PR property if

$$T_0(z) = z^{-D} \text{ and } T_l(z) = 0 \quad \text{for } l = 1,\ 2,\ \ldots,\ M-1$$

For the sake of detailed exposition of the new design technique in the rest of the paper our attention is focused on the class of *orthoonal* CMFBs, namely those where the prototype filter is of linear phase. Under the circumstance, the system delay D is equal to $N-1$; the analysis and synthesis filters are related by $g_k(n) = h_k(N-n-1)$; and the design variables are merely the components in the first half of $p(n)$'s, i.e.,

$$\boldsymbol{p} = [p(0)\ \ p(1)\ \ \cdots\ \ p(\frac{N}{2}-)]^T$$

The time-domain version of the aforementioned PR conditions is a set of second-order algebraic equations given by

$$\boldsymbol{p}^T\boldsymbol{Q}_{l,n}\boldsymbol{p} = c_n$$

for $l = 0,\ 1,\ \ldots,\ M/2-1$ and $n = 0,\ 1,\ \ldots,\ m-1$ with $m = 0.5N/M$, where

$$\boldsymbol{Q}_{l,n} = \boldsymbol{V}_l\boldsymbol{J}\boldsymbol{D}_n\boldsymbol{V}_l^T + \boldsymbol{V}_{l+M}\boldsymbol{J}\boldsymbol{D}_n\boldsymbol{V}_{l+M}^T$$

and $\boldsymbol{V}_l \in R^{N/2\times m}$, $\boldsymbol{J} \in r^{m\times m}$, $\boldsymbol{D}_n \in R^{m\times m}$, and c_n are defined as

$$\boldsymbol{V}_l(i,j) = \begin{cases} 1 & \text{if } i = l+2jM \text{ and } l+2jM < mM, \\ \text{or} & \text{if } i = N-1-l-2jM,\ l+2jM \geq mM \\ 0 & \text{otherwise} \end{cases}$$

$$\boldsymbol{J} = \text{flipud}(\boldsymbol{I}_m),\ \ \boldsymbol{D}_n(i,j) = \begin{cases} 1 & \text{if } i+j = n \\ 0 & \text{otherwise} \end{cases}$$

and $c_n = 0.5\delta(n)/M$ [7].

A common formulation for the design of orthogonal PR CMFBs seeks a lowpass prototype FIR filter $P(z)$ with minimum stopband energy subject to the PR conditions [14][18], where the stopband energy is defined by

$$e_2(\boldsymbol{p}) = \int_{\omega_s}^{\pi} |P(e^{j\omega})|^2 d\omega$$

where $\omega_s = \pi/M$. By writing $P(e^{j\omega}) = 2\boldsymbol{p}^T\boldsymbol{c}(\omega)$ with $\boldsymbol{c}(\omega) = [\cos(\frac{N-1}{2})\omega\ \ \cos(\frac{N-3}{2})\omega\ \cdots\ \cos(\frac{\omega}{2})]^T$, the stopband energy becomes

$$e_2(\boldsymbol{p}) = \boldsymbol{p}^T\boldsymbol{W}\boldsymbol{p},\ \ \boldsymbol{W} = 4\int_{\pi/M}^{\pi} \boldsymbol{c}(\omega)\boldsymbol{c}(\omega)^T d\omega$$

and the design problem at hand boils down to solving the QP problem

$$\text{minimize } \ e_2(\boldsymbol{p}) = \boldsymbol{p}^T\boldsymbol{W}\boldsymbol{p} \tag{1a}$$

$$\text{subject to: } \boldsymbol{p}^T\boldsymbol{Q}_{l,n}\boldsymbol{p} = c_n, \tag{1b}$$

where $0 \leq l \leq M/2-1;\ \ 0 \leq n \leq m-1$.

III. Convex Formulation via Improved Constraint Linearization

A. Convex Formulation via Constraint Linearization

The quadratic objective function in (1a) is convex because matrix $\boldsymbol{W}$ is positive definite. However, the quadratic equality constraints in (1b) are not convex and hence (1) is a nonconvex QP problem, admitting multiple local minimizers, many of which provide only suboptimal performance. Under the circumstances, to solve (1) it is natural and effective to develop a method that takes the advantage of having a convex objective function and iteratively solves a sequence of *convex* QP problems, each minimizes the same convex $e_2(\boldsymbol{p})$ subject to a set of convex constraints that approximate and gradually converge to the original nonconvex constraints in (1b).

In the literature, the constraints in (1b) are approximated by an iterate-dependant linearization as follows. Let the kth iterate be $\boldsymbol{p}_k$ which is updated in the kth iteration to $\boldsymbol{p}_{k+1} = \boldsymbol{p}_k + \boldsymbol{\delta}_k$ where $\boldsymbol{\delta}_k$ solves the QP problem

$$\underset{\delta}{\text{minimize}} \quad e_2(\boldsymbol{p}_k+\boldsymbol{\delta}) = (\boldsymbol{p}_k+\boldsymbol{\delta})^T\boldsymbol{W}(\boldsymbol{p}_k+\boldsymbol{\delta}) \tag{2a}$$

$$\text{subject to:} \quad (\boldsymbol{p}_k+\boldsymbol{\delta})^T\boldsymbol{Q}_{l,n}(\boldsymbol{p}_k+\boldsymbol{\delta}) = c_n \tag{2b}$$

where $0 \leq l \leq M/2-1$ and $0 \leq n \leq m-1$. With respect to variable $\boldsymbol{\delta}$, the objective function in (2a) remains quadratic and convex. We now write each constraint in (2b) as

$$\boldsymbol{p}_k^T\hat{\boldsymbol{Q}}_{l,n}\boldsymbol{\delta} + \boldsymbol{\delta}^T\boldsymbol{Q}_{l,n}\boldsymbol{\delta} = \hat{c}_n \tag{3}$$

where $\hat{\boldsymbol{Q}}_{l,n} = \boldsymbol{Q}_{l,n} + \boldsymbol{Q}_{l,n}^T$ and $\hat{c}_n = c_n - \boldsymbol{p}_k^T\boldsymbol{Q}_{l,n}\boldsymbol{p}_k$. In [14] and [18], the nonconvex constraint in (3) is linearized by dropping the term $\boldsymbol{\delta}^T\boldsymbol{Q}_{l,n}\boldsymbol{\delta}$, yielding

$$\boldsymbol{p}^T\hat{\boldsymbol{Q}}_{l,n}\boldsymbol{\delta} \approx \hat{c}_n,\ 0 \leq l \leq M/2-1,\ 0 \leq n \leq m-1 \tag{4}$$

The error induced by above linear approximation in an individual quadratic constraint is $\boldsymbol{\delta}^T\boldsymbol{Q}_{l,n}\boldsymbol{\delta}$ which is negligible when the algorithm converges and hence $\boldsymbol{\delta}$ approaches zero because the error then possesses a second-order smallness in a linear (first-order) approximation. Therefore, the linear constraint in (4) is asymptotically equivalent to the original constraint in (3) hence (2b). Nevertheless, there are better ways in the dealings with the second-order term $\boldsymbol{\delta}^T\boldsymbol{Q}_{l,n}\boldsymbol{\delta}$. In what follows we present two techniques of this kind.

Rather than dropping $\boldsymbol{\delta}^T\boldsymbol{Q}_{l,n}\boldsymbol{\delta}$, the first technique is to replace it in (3) by $\boldsymbol{\delta}_{k-1}^T\boldsymbol{Q}_{l,n}\boldsymbol{\delta}_{k-1}$ where $\boldsymbol{\delta}_{k-1}$ denotes the optimized $\boldsymbol{\delta}$ obtained in the $(k-1)$th iteration. The replacement yields a linear approximation of constraint (3) as

$$\boldsymbol{p}_k^T\hat{\boldsymbol{Q}}_{l,n}\boldsymbol{\delta} \approx \tilde{c}_n, \quad 0 \leq l \leq M/2-1 \text{ and } 0 \leq n \leq m-1 \tag{5}$$

where $\tilde{c}_n = c_n - \boldsymbol{p}_k^T\boldsymbol{Q}_{l,n}\boldsymbol{p}_k - \boldsymbol{\delta}_{k-1}^T\boldsymbol{Q}_{l,n}\boldsymbol{\delta}_{k-1}$. The error induced by (5) is equal to $\boldsymbol{\delta}^T\boldsymbol{Q}_{l,n}\boldsymbol{\delta} - \boldsymbol{\delta}_{k-1}^T\boldsymbol{Q}_{l,n}\boldsymbol{\delta}_{k-1}$ which obviously goes to zero much quicker than that induced by (4), namely $\boldsymbol{\delta}^T\boldsymbol{Q}_{l,n}\boldsymbol{\delta}$, when the algorithm converges.

Alternatively, the term $\boldsymbol{\delta}^T\boldsymbol{Q}_{l,n}\boldsymbol{\delta}$ in (3) may be replaced by $\boldsymbol{\delta}_{k-1}^T\boldsymbol{Q}_{l,n}\boldsymbol{\delta}$ that yields yet another linear approximation

$$(\boldsymbol{p}_k+\boldsymbol{\delta}_{k-1})^T\tilde{\boldsymbol{Q}}_{l,n}\boldsymbol{\delta} \approx \hat{c}_n,\ 0 \leq l \leq M/2-1,\ 0 \leq n \leq m-1 \tag{6}$$

The approximation error induced by (6) is now reduced from $\boldsymbol{\delta}^T \boldsymbol{Q}_{l,n}\boldsymbol{\delta}$ to $(\boldsymbol{\delta} - \boldsymbol{\delta}_{k-1})^T \hat{\boldsymbol{Q}}_{l,n}\boldsymbol{\delta}$. The error has an upper bound $\kappa \cdot \|\boldsymbol{\delta} - \boldsymbol{\delta}_{k-1}\|_2 \|\boldsymbol{\delta}\|_2$ where κ is a constant (related to the norm of $\hat{\boldsymbol{Q}}_{l,n}$) and, when the algorithm converges, $\|\boldsymbol{\delta} - \boldsymbol{\delta}_{k-1}\|_2/\|\boldsymbol{\delta}\|_2$ goes to zero. Therefore, we have

$$(\boldsymbol{\delta} - \boldsymbol{\delta}_{k-1})^T \hat{\boldsymbol{Q}}_{l,n}\boldsymbol{\delta} = o(\|\boldsymbol{\delta}\|_2^2)$$

We reiterate that the new approximations in (5) and (6) remain linear and hold the desired asymptotical equivalence to the original constraints in (2b). On comparing with the approximation scheme in (4), the additional computations required by (5) (calculating $\boldsymbol{\delta}_{k-1}\boldsymbol{Q}_{l,n}\boldsymbol{\delta}_{k-1}$ to get $\tilde{c}_n$) and (6) (adding $\boldsymbol{\delta}_{k-1}$ to $\boldsymbol{p}_k$) are fairly insignificant relative to the rest of the computational effort required by the algorithm (see below for details). We also remark that other convex approximations of constraint (3) exist, however these are quadratic approximations which lead to a QP problem with considerably increased complexity.

For the sake of clarity, below we describe a design algorithm that employs scheme (6). There are a total of $Mm/2$ (which by definition is equal to $N/4$) linear constraints in (6) which can be put together and expressed compactly as $\boldsymbol{A}_k\boldsymbol{\delta} = \hat{\boldsymbol{c}}$ where $\boldsymbol{A}_k \in R^{N/4\times N/2}$ and $\hat{\boldsymbol{c}} \in R^{N/4\times 1}$ are known. In the kth iteration where $\boldsymbol{p}_k$ is a known iterate, we solve the convex QP problem

$$\underset{\delta}{\text{minimize}} \quad e_2(\boldsymbol{p}_k + \boldsymbol{\delta}) = (\boldsymbol{p}_k + \boldsymbol{\delta})^T \boldsymbol{W}(\boldsymbol{p}_k + \boldsymbol{\delta}) \tag{7a}$$

$$\text{subject to:} \quad \boldsymbol{A}_k\boldsymbol{\delta} = \hat{\boldsymbol{c}} \tag{7b}$$

Eq. (7b) possesses infinitely many solutions and the entire set of solutions of (7b) can be characterized as $\boldsymbol{\delta} = \boldsymbol{V}_e\boldsymbol{\phi} + \boldsymbol{\delta}_s$ where $\boldsymbol{\delta}_s$ is a special solution of (7b), $\boldsymbol{V}_e \in R^{N/2\times N/4}$ consists of $N/4$ basis vectors of the null space of $\boldsymbol{A}_k$, and $\boldsymbol{\phi} \in R^{N/4}$ is a vector containing $N/4$ free parameters, and techniques based on QR or singular value decomposition for computing $\boldsymbol{\delta}_s$ and $\boldsymbol{V}_e$ are available in the literature [20]. By substituting $\boldsymbol{\delta} = \boldsymbol{V}_c\boldsymbol{\phi} + \boldsymbol{\delta}_s$ into (7a), (7) becomes an unconstrained problem with respect to $\boldsymbol{\phi}$, namely,

$$\underset{\phi}{\text{minimize}}\, \boldsymbol{\phi}^T \hat{\boldsymbol{W}}\boldsymbol{\phi} + 2\boldsymbol{\phi}^T\boldsymbol{b} + \text{const} \tag{8}$$

where $\hat{\boldsymbol{W}} = \boldsymbol{V}_e^T\boldsymbol{W}\boldsymbol{V}_e$ and $\boldsymbol{b} = \boldsymbol{V}_e^T\boldsymbol{W}(\boldsymbol{p}_k + \boldsymbol{\delta}_s)$. By definition, matrix $\hat{\boldsymbol{W}}$ is positive define and hence (8) is a convex QP whose global minimizer is equal to the unique stationary point of its objective function, namely

$$\boldsymbol{\phi}^* = -\hat{\boldsymbol{W}}^{-1}\boldsymbol{b} \tag{9}$$

The solution of (7) is given by $\boldsymbol{\delta}^* = \boldsymbol{V}_e\boldsymbol{\phi}^* + \boldsymbol{\delta}_s$.

B. Implementation Issues

(a) In our algorithm, the minimum 2-norm solution of $\boldsymbol{A}_k\boldsymbol{\delta} = \hat{\boldsymbol{c}}$ was taken to be the special solution $\boldsymbol{\delta}_s$. That is, $\boldsymbol{\delta}_s = \boldsymbol{A}_k^\dagger\hat{\boldsymbol{c}}$ where $\boldsymbol{A}_k^\dagger$ is the Moore-Penrose pseudo-inverse of $\boldsymbol{A}_k$.

(b) To implement the linearization scheme in (6) at the beginning of the iteration, i.e. at $k = 0$, the term $\boldsymbol{\delta}_{k-1}$ is set to zero. In addition, since during the first a few iterations $\boldsymbol{\delta}_{k-1}$ is far from optimal, the scheme was found to be more stable if the term $\boldsymbol{\delta}_{k-1}$ is gradually induced. As a result, in practice (6) is slightly modified to

$$(\boldsymbol{p}_k + \gamma_k\boldsymbol{\delta}_{k-1})^T \hat{\boldsymbol{Q}}_{l,n}\boldsymbol{\delta} \approx \hat{c}_n \tag{10}$$

where γ_k is set to zero at $k = 0$ and monotonically approach a constant $\gamma \leq 1$.

(c) The third issue has to do with the validity of the linearization schemes in (6) (and hence (10)). That is, the scheme is valid only if $\boldsymbol{\delta}$ remains small. As in [18], this smallness is monitored in terms of $\|\boldsymbol{\delta}^*\|_2/\|\boldsymbol{p}_k\|$: if it does not exceeds a certain threshold ε, then compute the next $\boldsymbol{\delta}^*$ using (9); otherwise, compute $\boldsymbol{\delta}^*$ using

$$\boldsymbol{\phi}^* = -\hat{\boldsymbol{W}}^{-1}\hat{\boldsymbol{b}} \tag{11}$$

where $\hat{\boldsymbol{b}} = \boldsymbol{V}_e^T\boldsymbol{W}\boldsymbol{\delta}_s$.

C. The Algorithm

The algorithm can now be summarized as follows.

Step 1
Input design parameters N M, ε, initial $\boldsymbol{p}_0$, and the number of iterations K. Set $k = 0$.

Step 2
If $k < K$, update $\boldsymbol{p}_k$ to $\boldsymbol{p}_{k+1} = \boldsymbol{p}_k + \boldsymbol{\delta}_k$, where matrix $\boldsymbol{A}_k$ is constructed using (10); $\boldsymbol{\delta}_k = \boldsymbol{V}_e\boldsymbol{\phi}^* + \boldsymbol{\delta}_s$ with $\boldsymbol{\phi}^*$ is computed using (9) or (11); and $\boldsymbol{\delta}_s = \boldsymbol{A}_k^\dagger\hat{\boldsymbol{c}}$. Set $k := k+1$ and repeat this step.

Step 3
If $k = K$, output $\boldsymbol{p}_K$ as the solution.

IV. An Design Example

For illustration, the proposed algorithm was applied to design a 16-channel orthogonal PR CMFB of length $N = 384$. This implies that $M = 16$ and $m = 12$. The threshold ε (see Sec. III.B) was set to 10^{-11} and γ_k in (10) was set to $1 - 1/(1 + k)$ so that it starts from value zero at $k = 0$ and monotonically approaching unity as iteration proceeds. It took the algorithm 95 iterations to reach a linear-phase FIR prototype filter with satisfactory performance. The design performance of the optimal design $\boldsymbol{p}^*$ is evaluated in terms of stopband energy $e_2(\boldsymbol{p}^*)$ of the prototype filter, magnitude distortion defined by

$$e_m(\omega) = 1 - |T_0(e^{j\omega})| \quad \text{for } \omega \in [0,\ \pi]$$

and the total aliasing distortion (in dB) defined by

$$e_{ta}(\omega) = 10\log_{10}\left(\sum_{l=1}^{M-1} |T_l(e^{j\omega})|^2\right) \quad \text{for } \omega \in [0,\ \pi]$$

In addition to these frequency-domain measures, the PR property of $\boldsymbol{p}^*$ is also evaluated in terms of its satisfaction of the time-domain constraints (1b), namely

$$e_{PR} = \sqrt{\frac{2}{Mm}}\left[\sum_{l=0}^{\frac{M}{2}-1}\sum_{n=0}^{m-1}(\boldsymbol{p}^{*T}\boldsymbol{Q}_{l,n}\boldsymbol{p}^* - c_n)^2\right]^{1/2}$$

The magnitude responses of the optimal prototype filter $P(z)$ and the 16 analysis filters; magnitude distortion $e_m(\omega)$; and the total aliasing distortion $e_m(\omega)$ are depicted in Fig. 1(a), (b), (c), and (d), respectively. The stopband energy of the prototype filter was found to be $e_2(\boldsymbol{p}^*) = 1.31 \times 10^{-10}$ and the time-domain PR error was $e_{PR} = 9.35 \times 10^{-21}$. The order of smallness of e_{PR} implies that all constraints in (1b) were satisfied with high accuracy and hence $\boldsymbol{p}^*$ defines a PR CMFB. For comparison, a state-of-the-art design of an orthogonal PR CMFB with the same design specifications can be found in [18]. The design reported in [18] yielded $e_2(\boldsymbol{p}^*) = 3.52 \times 10^{-10}$; its $e_m(\omega)$ and $e_{ta}(\omega)$ can be found in Fig. 1 of [18] which shows a comparable $e_{ta}(\omega)$ but a larger $e_m(\omega)$ (varying in the vicinity of 3.3×10^{-13}).

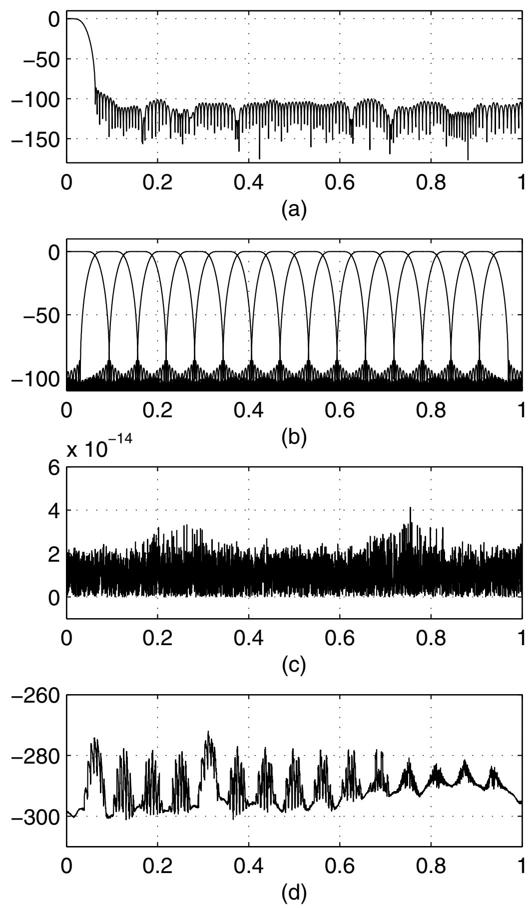

Fig. 1. Magnitude responses of (a) prototype $P(z)$ and (b) analysis filters, (c) magnitude distortion $e_m(\omega)$, (d) total aliasing distortion $e_{ta}(\omega)$ in dB.

V. Conclusion

New linearization schemes for time-domain quadratic constraints in a QP formulation for the design of orthogonal PR CMFBs are proposed and analyzed. A design example is presented to demonstrate effectiveness of the design technique. With straightforward modifications, the proposed algorithm is applicable to the class of biorthogonal CMFBs.

References

[1] R. D. Koilpillai and P. P. Vaidyanathan, Cosine-modulated FIR filter banks satisfying perfect reconstruction, *IEEE Trans. Signal Process.*, vol. 40, pp. 770-783, Apr. 1992.

[2] T. Saramki, "Designing prototype filters for perfect reconstruction cosine-modulated filter banks, *IEEE Int. Symp. Circuits Syst.*, vol. 3, pp. 1605–1608, San Diego, CA., May 1992.

[3] P. P. Vaidyanathan, Multirate Systems and Filter Banks. Prentice-Hall, 1993.

[4] C. D. Creusere and S. K. Mitra, "A simple method for designing high quality prototype filters for M-band pseudo QMF banks," *IEEE Trans. Signal Process.*, vol. 43, pp. 1005–1007, Apr. 1995.

[5] T. Q. Nguyen, "Digital filter bank design quadratic-constrained formulation, *IEEE Trans. Signal Process.*, vol. 43, pp. 2103–2108, Sep. 1995.

[6] Y.-P. Lin and P. P. Vaidyanathan, "Linear phase cosine modulated maximally decimated filter banks with perfect reconstruction", *IEEE Trans. Signal Process.*, vol. 43, pp. 2525–2539, Nov. 1995.

[7] T. Q. Nguyen and R. D. Koilpillai, "The theory and design of arbitrary-length cosine modulated filter banks and wavelets, satisfying perfect reconstruction", *IEEE Trans. Signal Process.*, vol. 44, pp. 473–483, Mar. 1996.

[8] T. Q. Nguyen and P. N. Heller, "Biorthogonal cosine-modulated filter banks", *IEEE Int. Conf. Acoustics, Speech, and Signal Process.*, vol. 3, pp. 1471–1474, Atlanta, GA, May 1996.

[9] H. Xu, W.-S. Lu, and A. Antoniou, "Efficient iterative design method for cosine-modulated QMF banks", *IEEE Trans. Signal Process.*, vol. 44, pp. 1657–1668, July 1996.

[10] G. Schuller, "A new factorization and structure for cosine modulated filter banks with variable system delay", *Asilomar Conf. Signals, Systems, and Computers, Pacific Glove*, CA, vol. 2, pp. 1310–1314, Nov. 1996.

[11] P. N. Heller, T. Karp, and T. Q. Nguyen, "A general formulation of modulated filter banks", *IEEE Trans. Signal Process.*, vol. 47, pp. 986–1002, Apr. 1999.

[12] T. Karp, A. Mertins, and G. Schuller, "Efficient biorthogonal cosine-modulated filter banks", *Signal Process.*, vol. 81, pp. 997–1016, May 2001.

[13] R. Bregovi and T. Saramki, "An efficient approach for designing nearly perfect-reconstruction low-delay cosine-modulated filter banks", *IEEE Int. Symp. Circuits Syst.*, Scottsdale, AZ, vol. 1, pp. 825–828, May 2002.

[14] W.-S. Lu, T. Saramki, and R. Bregovi, "Design of practically perfect-reconstruction cosine-modulated filter banks: A second-order cone programming approach," *IEEE Trans. Circuits Syst. I*, vol. 51, pp. 552–563, Mar. 2004.

[15] M. F. Furtado, Jr., P. S. R. Diniz, and S. L. Netto, "Numerically efficient optimal design of cosine-modulated filter banks with peak-constrained least-squares behavior," *IEEE Trans. Circuits Syst. I*, vol. 52, pp. 597–608, Mar. 2005.

[16] H. H. Kha and T. Q. Nguyen, "Efficient design of cosine-modulated filter banks via convex optimization," *IEEE Trans. Signal Process.*, vol. 57, pp. 966–976, Mar. 2009.

[17] J. Yan and W.-S. Lu, "Global design of perfect-reconstruction orthogonal cosine-modulated filter banks," in *Proc. CCECE*, Calgary, AB, Canada, May 2010.

[18] G. Doblinger, "A fast design method for perfect-reconstruction uniform cosine-modulated filter banks," *IEEE Trans. Signal Process.*, vol. 60, no. 12, pp. 6693–6697, Dec. 2012.

[19] J.-J. Lee and B. G. Lee, "A design of nonuniform cosine modulated filter banks," *IEEE Trans. Circuits Syst. II*, vol. 42, no. 11, pp. 732–737, Nov. 2005.

[20] A. Antoniou and W.-S. Lu, *Practical Optimization: Algorithms and Engineering Applications*, Springer, 2007.